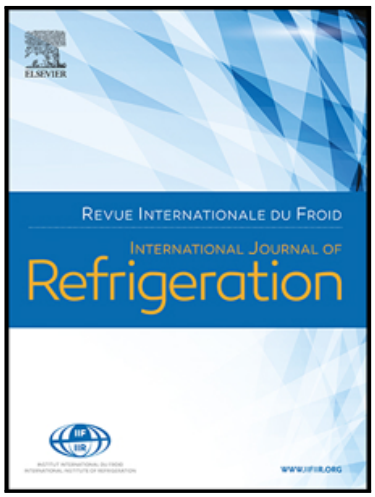

Experimental study of a novel cool-storage refrigerator with controllable two-phase loop thermosyphon

Weixin Liu , Chuxiong Chen , Jingyu Cao , Lijun Wu , Wei Ren , Dongsheng Jiao , Gang Pei

PII: S0140-7007(21)00134-1
DOI: https://doi.org/10.1016/j.ijrefrig.2021.04.009
Reference: JIJR 5103

To appear in: *International Journal of Refrigeration*

Received date: 10 December 2020
Revised date: 25 March 2021
Accepted date: 11 April 2021

Please cite this article as: Weixin Liu , Chuxiong Chen , Jingyu Cao , Lijun Wu , Wei Ren , Dongsheng Jiao , Gang Pei , Experimental study of a novel cool-storage refrigerator with controllable two-phase loop thermosyphon, *International Journal of Refrigeration* (2021), doi: https://doi.org/10.1016/j.ijrefrig.2021.04.009

Experimental study of a novel cool-storage refrigerator with controllable two-phase loop thermosyphon

Weixin Liu[a], Chuxiong Chen[b], Jingyu Cao[c*], Lijun Wu[a], Wei Ren[d], Dongsheng Jiao[a], Gang Pei[a,*]

[a] *Department of Thermal Science and Energy Engineering, University of Science and Technology of China, 96 Jinzhai Road, Hefei, China*

[b] *Hunan Central South Intelligent Equipment Co.,Ltd., Changsha 410117, China*

[c] *College of Civil Engineering, Hunan University, Changsha 410082, China*

[d] *Hefei Hualing Co., Ltd., Hefei 230601, China*

[*]Corresponding author. Email address: peigang@ustc.edu.cn; jycao@hnu.edu.cn

Keywords
Thermosyphon; Refrigerator; Temperature control; Cool storage

Abstract:

Cool storage has been considering an efficient and cost-effective means to enhance the behavior of a refrigerator. However, its drawback in temperature control of the refrigerator compartment has not received enough attention. The controllable two-phase loop thermosyphon has the prospect of solving this problem. In this study, a novel cool-storage refrigerator integrated with a controllable two-phase loop thermosyphon is built to investigate its precise temperature control capacity. The phase change material is optimized by the orthogonal experiment method. The controllable two-phase loop thermosyphon presents the optimal cooling performance for the fresh food compartment when the filling ratio is 27.0%. As the average temperature of the fresh food compartment increases, the one on-off cycle of the controllable two-phase loop thermosyphon maintains at 32 min, and the operation ratio varies from 86.3% to 13.6%. The temperature control accuracy can be improved from 2.1 °C to 0.6 °C and the overall time of one on-off cycle decreases from 49.8 min to 22.4 min. The operation ratio gradually increases from 7.2% to 38.56% as the ambient temperatures increase. The results demonstrate that the controllable two-phase loop thermosyphon is a feasible and effective way to improve the temperature control performance of the cool-storage refrigerator.

***Keywords**:* thermosyphon, refrigerator, temperature control, cool storage

Nomenclature

CTPLT	controllable two-phase loop thermosyphon	*ave*	average value over time
P	pressure, MPa	*top*	top cabinet of the fresh food compartment
T	temperature, °C	*mid*	middle cabinet of the fresh food compartment
L	length, m	*btm*	bottom cabinet of the fresh food compartment
PCM	phase change material	*diff*	temperature difference
DSC	differential scanning calorimetry		
R	filling ratio of R407c		
V'	volume of the liquid R407c, m^3		
V_{CTPLT}	volume of the CTPLT, m^3		
m'	mass of the liquid R407c, kg		
v'	specific volume of the liquid R407c, $m^3\ kg^{-1}$		

Greek letters

Y	calculated parameter
X	independent variable

Subscripts

fre	fresh food compartment

1. Introduction

Refrigerator has been widely used in the field of domestic appliances and has become a major consumer of household electricity. Efficiency improvement of refrigerators is of great importance to global energy-saving. Generally, the energy-saving performance of refrigerators can be improved by the modification of compressor and insulation, the optimization of the control strategy of the system, etc. In recent years, phase change material (PCM) have received considerable attention in various industries, such as thermal energy storage system (Vikram et al., 2019), air conditioning system (Zou et al., 2018), energy-saving in buildings (Alam et al., 2019), cooling of electronic devices (Zhu et al., 2020), and solar fields (Nasef et al., 2019). Recently, researches have been conducted to investigate

the feasibility of the applications of PCM to improve the performance of the refrigeration systems, especially in the domestic refrigerator. The refrigerator with PCM has great prospects in saving energy (Omara and Mohammedali, 2020) and promoting the energy efficiency of the refrigerators (Maiorino et al., 2020).

In the past few years, tremendous efforts have been made to study the performance of the refrigerators combined with PCM. Pirvaram et al. arranged two eutectic PCMs on the back of the condenser along the refrigerant flow direction, and the energy consumption was reduced by 13% compared with that of the original refrigerator (Pirvaram et al., 2019). In another work, Marques et al. designed a novel thermal energy storage refrigerator using water as the PCM. The experimental results demonstrated that the temperature of the refrigerator compartment could maintain below 5 °C for 3-5 h when 1 kg of the PCM was coupled with the evaporator (Marques et al., 2014). Niyaj et al. found that the temperature range of the refrigerator compartment could maintain at 2-3 °C by locating the PCMs in the newly designed evaporator, which is better than the 6-8 °C of the traditional refrigerator without PCM (Niyaj and Sapali, 2017). Elarem et al. demonstrated that the novel refrigerator with a PCM heat exchanger can save energy consumption by 12% and increase the COP by 8% as compared with the original refrigerator (Elarem et al., 2017). Yusufoglu et al. built refrigerator prototypes to investigate the energy-saving performance of a refrigerator integrating with different kinds of PCMs, and the experimental results demonstrated that the best energy-saving of the refrigerator prototype is 9.4% (Yusufoglu et al., 2015). Besides the experimental investigations, theoretical investigations via mathematical models have also been reported. For example, Bakhshipour established a mathematical model to simulate the performance of a refrigerator with the PCM located at the outlet of the condenser. The simulation results indicated that the usage of

PCM decreased the outlet refrigerant temperature of the condenser which lead to an increase in COP to 9.58% (Bakhshipour et al., 2017). All these reports demonstrate that the combination of PCM and refrigerator can improve the COP or maintain a low temperature of the compartment. It is well known that the temperature control of the refrigerator compartment has a great effect on the food quality, but studies on the precise temperature control of the cool-storage refrigerator have not received enough attention.

As an energy-efficient heat transfer device, the two-phase loop thermosyphon, which can also be called as two-phase closed loop-thermosyphon (Tecchio et al., 2017), thermosiphon loop (Chauhan and Kandlikar, 2019), loop thermosyphon (Kiseev and Sazhin, 2019), or two-phase thermosyphon loop (Khodabandeh, 2005), is a promising technology to solve the problem associated with the precise temperature control of the cool-storage refrigerator. The gravity and temperature difference drives the internal heat transfer and flow of the working fluid of the two-phase loop thermosyphon (Cao et al., 2020b). The two-phase loop thermosyphon has been considered as a highly efficient heat transfer device because of its excellent characteristics, such as simple structure, low cost, and low heat transfer resistance (Hong et al., 2018). The two-phase loop thermosyphon can be used in the cooling of data centers (Yue et al., 2019), seasonal cold storage system (Li et al., 2020), air-conditioning system (Yan et al., 2016), energy-efficient building (Cao et al., 2020a), nuclear reactor (Fu et al., 2015), and so on. It can also be used in solar fields like conventional solar water heater (Zhang et al., 2020) and the cooling of concentrating solar cells (Chen and Yang, 2016).

Up to now, a lot of researches on the two-phase loop thermosyphon have been conducted. The first aspect is to improve the behaviors of the two-phase loop thermosyphon (Cao et al., 2019). Zhang et al. performed long-term tests to optimize the filling ratio of the two-phase loop thermosyphon that

is coupled with photovoltaic/thermal (PV/T) system, and better energy efficiency and exergy efficiency were obtained when the filling ratio was about 32% (Zhang et al., 2019). Kondou et al. conducted experiments to improve the dissipation of the two-phase loop thermosyphon using R134a, R1234ze (E), and R1234ze (Z) with a super-hydrophilic boiling surface, and the heat flux was extended to 1600, 1400, and 1300 kW m^{-2}, respectively (Kondou et al., 2017). Shao et al. designed a novel two-phase loop thermosyphon with an evaporative condenser to cool the data center, the results indicated that the annual free cooling was extended by 7%-14% compared with conventional loop thermosyphon (Shao et al., 2019). He et al. designed a two-phase loop thermosyphon using a mixed-wettability evaporator surface, which exhibited the heat transfer coefficient with twice that of the copper mirror surface (He et al., 2017). In recent years, the internal heat transfers and flow characteristics of the two-phase loop thermosyphon have also been investigated. Tong et al. reported that the R744 two-phase thermosyphon loop experienced prestart, oscillatory, and stable state with the increase of the heat load (Tong et al., 2017). Zhang et al. established a simulation model of the thermosyphon integrated with mechanical refrigeration, demonstrating that the circulation flow rates increased with the increase of height difference between evaporator and condenser but the increase is negligible when the height difference is higher than 0.5 m (Zhang et al., 2017). Zhang et al. investigated the internal flow characteristics in the downcomer of the two-phase loop thermosyphon, the experimental results indicated the downcomer of the two-phase loop thermosyphon could be fully charged or partially charged as the working conditions changed (Zhang et al., 2015). Elkholy et al. reported that geyser instabilities resulting from the geyser boiling phenomenon of the two-phase loop thermosyphon were more pronounced for high filling ratio and low powers, but the effect of evaporator design on geyser instabilities was small (Elkholy and Kempers, 2020). Liu et al.

performed experiments to study the heat transfer and instability characteristics of a two-phase loop thermosyphon with a wide range of filling ratios. It indicated that the heat transfer was enhanced if the filling ratio decreased for a higher part of latent heat, but the adverse effect of evaporator dry-out and the geyser boiling instability will increase as well (Liu et al., 2019).

From the aforementioned literatures, the application scenarios of the two-phase loop thermosyphon were diversified in a variety of fields (Jafari et al., 2016), and the working characteristics have been fully investigated from different views (Bai et al., 2019). However, most researches focus on the passive heat transfer of the two-phase loop thermosyphon, which leads to poor temperature control and degrades the performance of the system. Studies on the precise temperature control by its active start-stop control are still rare. The practical temperature-control performance of the loop thermosyphon combined with phase change materials remains to be studied.

In this study, a novel cool-storage refrigerator with a controllable two-phase loop thermosyphon (CTPLT) was built to study its temperature control performance and the on-off control behaviors. The condenser of CTPLT is coupled with PCM, which is located in the freezer. Experiments were performed to select suitable PCM and the filling ratio of the CTPLT was optimized with the refrigerant of R407c. The temperature regulation performance and the on-off control behaviors of the CTPLT were examined at different temperatures of the fresh food compartment. The performances in the adjustment of temperature control accuracy and the on-off control behaviors of the CTPLT were systematically analyzed. Finally, the effects of ambient temperatures on the performance of the refrigerator were evaluated.

2. Experimental setup

2.1. Experimental apparatus and measurements

The novel cool-storage refrigerator with CTPLT is built based on a Media BCD-111 refrigerator, in which the fresh food compartment is located below the freezer. The experimental platform and the working principle of the system is shown in Fig. 1. The compressor refrigeration cycle only cools the freezer by adopting the original evaporator of the freezer. In addition, to further accelerate the cold storage process of the PCM, a serpentine copper tube that serves as an evaporator of the freezer is designed and is coupled with the PCM. The serpentine copper tube is connected with the original evaporator of the freezer in series. The length of the serpentine copper tube is 1.2 m, the corresponding outer diameter and inner diameter are 6.35 mm and 4.95 mm, respectively. Besides, the PCM and the condenser of the CTPLT are placed in a stainless box located in the freezer, and the PCM runs as the heat sink of the CTPLT. The detailed structures of the evaporator and condenser of the CTPLT are shown in Fig. 2. The original evaporator of the fresh food compartment is utilized as the evaporator of the CTPLT. The condenser section of the CTPLT consists of three parts: branch tubes, main tubes, and aluminum fins, where the branch tubes and fins are used for heat transfer enhancement. The operating states of the CTPLT are regulated by magnetic valves that are installed in the vapor and liquid lines, and the on-off state of the magnetic valves is controlled by the WK-206L temperature controller. When the magnetic valve is open, the liquid working fluid firstly receives heat from the fresh food compartment and evaporates in the evaporator of the CTPLT. The vapor working fluid enters the condenser along the vapor line and then condensates by heat transfer with the PCM. Thereafter, the liquid working fluid returns to the

evaporator along the liquid line. When the valve is closed, the internal two-phase circulation stops due to the resistance and the heat transfer level reaches zero. The heat transfer between the CTPLT and the fresh food compartment is actively controlled by the frequent start-stop of the CTPLT.

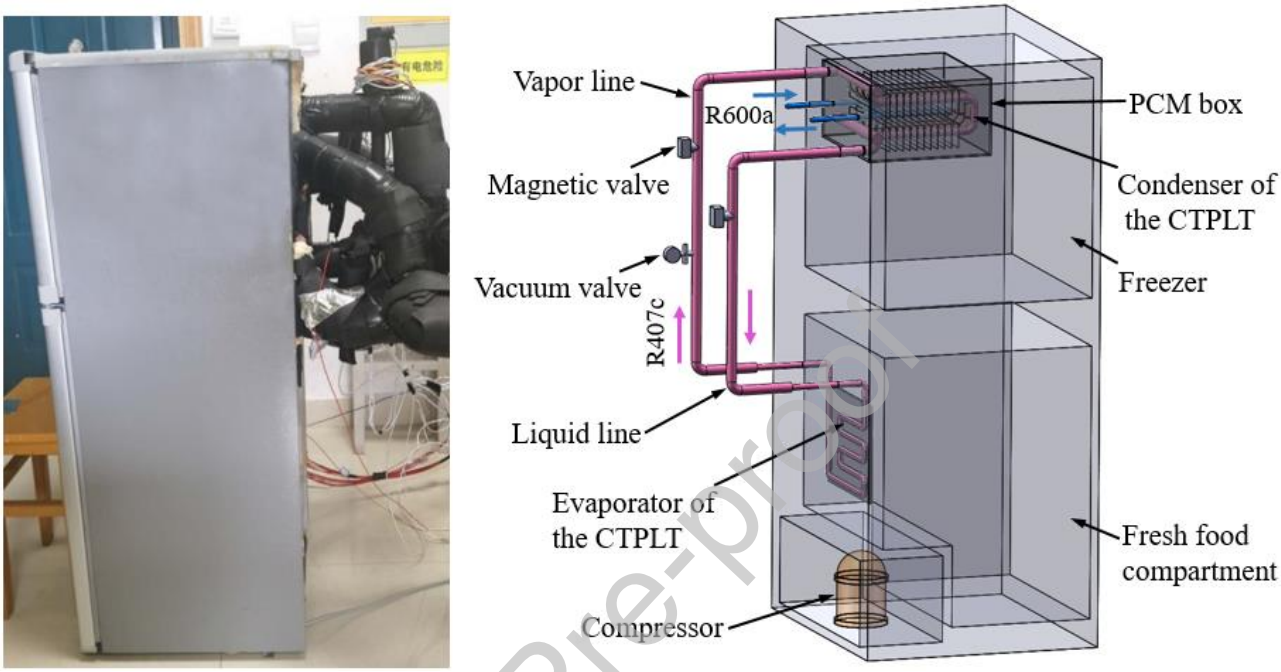

Fig. 1. The experiment platform and working principle of the system

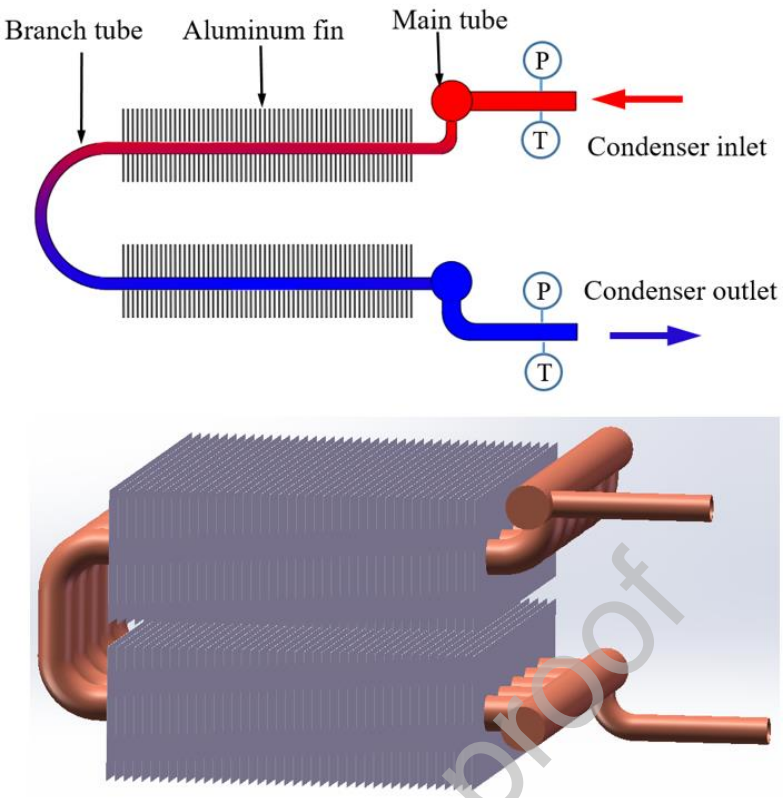

(a) Condenser of CTPLT

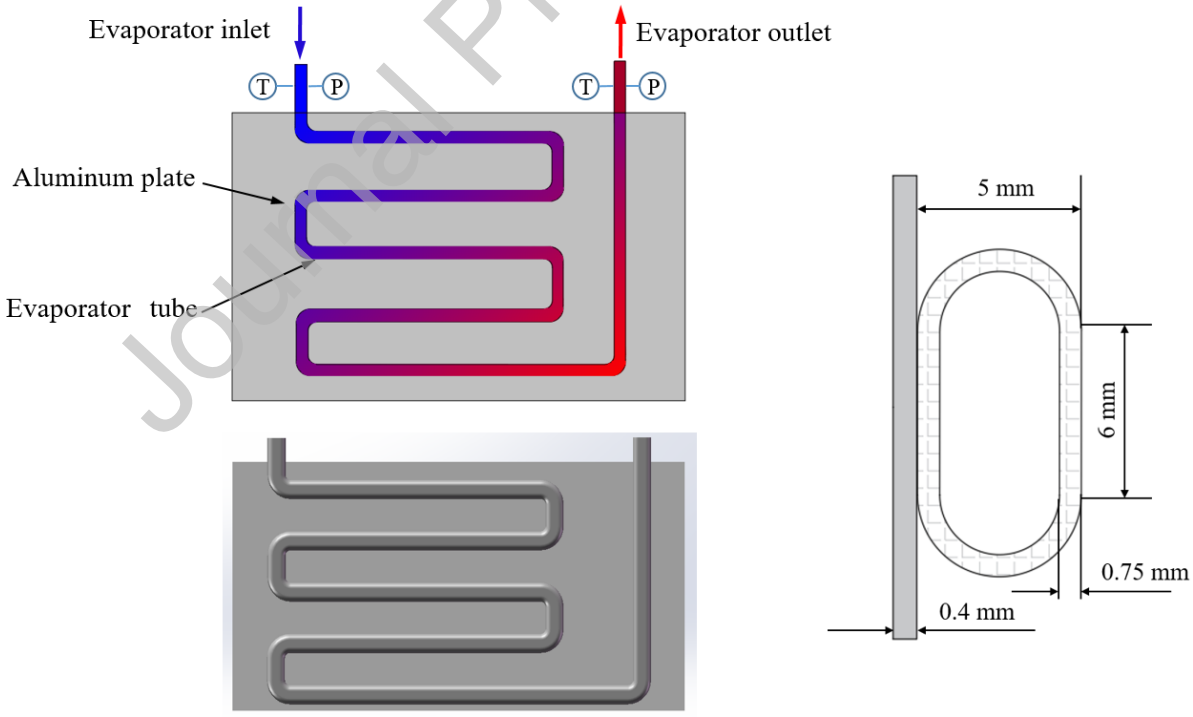

(b) Evaporator of CTPLT

Fig. 2. Main structure of CTPLT and its measurement points

For the established experimental platform, the relevant designed dimensions of components are described as follows: For the condenser of CTPLT, the lengths of the main tube and each branch tube are 0.25 m and 0.51 m, and the corresponding inner diameters are 14 mm and 8 mm, respectively. The lengths of the vapor line and liquid line are 0.94 m and 0.71 m, respectively, and the corresponding inner diameter is 10 mm. For the aluminum fins of the condenser, the length, width and thickness are 0.25 m, 0.05 m and 0.1 mm, respectively. For the evaporator of CTPLT, the cross-section is an oblateness. The detailed dimensions of the evaporator with a length of 1.3 m are shown in Fig. 2 (b). For the stainless box, the internal dimensions are 0.27 m×0.27 m×0.13 m with a wall thickness of 3 mm.

The measurements are shown in Fig. 2. Four WZP-291 Pt100 platinum resistances and four JT-131 pressure sensors are installed at the inlet and outlet of the condenser and evaporator to measure the temperatures and pressures of the working fluid. As shown in Fig. 3, three WZP-291 Pt100 platinum resistances that are inserted into three standard copper columns in the fresh food compartment are arranged to obtain the temperature data of the air. The appropriate hanging position for standard copper columns is adopted under the guidance of the national test standard of the domestic refrigerator. The ambient temperature is measured by the thermoelectric couples. During the experimental tests, the real-time measured data is collected by an Agilent data acquisition (Agilent 34970) and the data collection interval is 10 s. The vacuum valve, pressure gage (HONGSEN-466-NAH) and electronic scale (KFS-C1) are utilized to fill and discharge R407c. The temperature probe of the temperature controller (WK-206L) is arranged in the fresh food compartment, and the start-stop of the magnetic valve (HONGSEN 1064-4) is controlled by temperature feedback. The experimental apparatus and measurement devices are listed in Table 1.

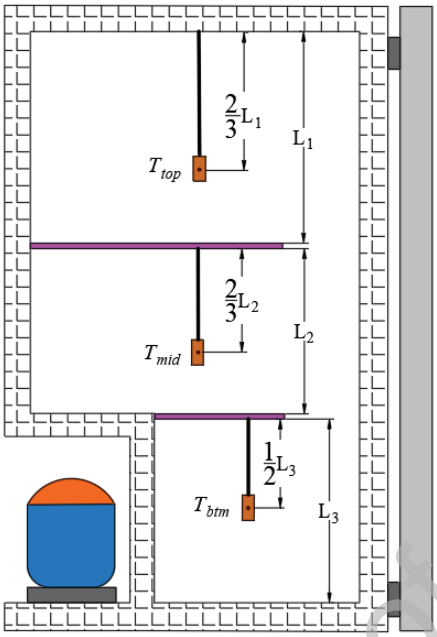

Fig. 3. Measurement points at the fresh food compartment

Table 1. List of experimental devices

Device	Specification	Range	Accuracy
Platinum resistance	WZP-291 Pt100	-40-100 °C	± 0.1 °C
Pressure sensor	JT-131	0-1000 kPa	± 5 kPa
Thermocouple	Type T	-200-350 °C	± 0.5 °C
Magnetic valve	HONGSEN 1064-4	/	/
Temperature controller	WK-206L	0-99 °C	± 0.1 °C
Electronic scale	KFS-C1	0-1 kg	± 0.5 g
Data acquisition unit	Agilent 34970	/	0.004%

2.2. Uncertainty analysis

The uncertainty analysis is conducted as follows. For the uncertainties of the measured parameters, the calibration errors of sensors are listed in Table 1. Besides, the filling ratio and temperature difference (T_{diff}) are calculated from other independent measured variables, The following calculation formula of uncertainty is commonly used (Watanabe et al., 2020):

$$\delta Y = \sqrt{\sum_{i=1}^{N}\left(\frac{\partial Y}{\partial X_i}\delta X_i\right)^2} \tag{1}$$

where Y the calculated parameter, X_i is independent variables, δX_i is the error of the measured variables. According to Eq. (1), the uncertainties of filling ratio and T_{diff} are 0.6% and 0.2 °C, respectively.

3. Experimental methods and calculation

The working fluid filling ratio of the designed CTPLT in this paper is defined as:

$$R = \frac{V'}{V_{CTPLT}} = \frac{m'v'}{V_{CT}} \tag{2}$$

where R is the filling ratio of the R407c; V' is the volume of the liquid R407c; V_{CTPLT} is the total volume of the CTPLT; m' and v' are the mass and specific volume of the liquid R407c, respectively.

The experiments are conducted in a testing room with precise temperature control. In the present work, the PCM is a kind of composite phase change material that is composed of three compounds: sodium chloride (NaCl), glycerol ($C_3H_8O_3$), and water, and the PCM is placed in the freezer compartment of a three-star level refrigerator so that the phase change temperature is under

-18 °C. Proper selections of the PCM are performed by orthogonal experiments and differential scanning calorimetry (DSC) to satisfy the requirements of phase change temperature and latent heat. Meanwhile, a comparative analysis of the temperature decreasing process of fresh food compartment using 50.0 g, 70.0 g, 90.0 g, 110.0 g, 130.0 g and 160.0 g R407c is performed, and the corresponding refrigerant filling ratios are 12.3%, 17.2%, 22.1%, 27.0%, 31.9%, and 39.3%, respectively. Following on the above experimental methods, experiments are conducted to systematically investigate the temperature control capacities of the designed refrigerator and the on-off behaviors of the CTPLT in different conditions. The main research procedures are as follows:

(1) Composite PCM with different composition ratios are formulated by the orthogonal experiments. One suitable PCM will be selected for the subsequent experiments.

(2) Comparative analysis of the temperature decreasing process of fresh food compartment at different refrigerant filling ratios of the CTPLT is performed, and the refrigerant filling ratio of the CTPLT is optimized.

(3) When the temperature control accuracy is given, the on-off behaviors of the CTPLT and the temperature regulation performance are analyzed at different fresh food compartment temperatures.

(4) When the temperature of the fresh food compartment is given, the variation of temperature control accuracy and operating characteristics of the CTPLT are studied in detail with different temperature controller settings.

(5) When the temperature of the fresh food compartment and the temperature control accuracy are given, the on-off characteristics of the CTPLT and the temperature variations of the fresh food compartment are tested at different ambient temperatures.

4. Results and discussion

4.1. PCM selection

The PCM studied in this work is placed in the freezer compartment of a three-star level refrigerator, and the temperature of the freezer compartment is under -18 °C according to the national standard, which means that the phase change temperature of the PCM should be below -18.0 °C. In the present work, the composite PCM is prepared by mixing NaCl, $C_3H_8O_3$ and water in a certain proportion. Considering the effect of different concentrations of NaCl and $C_3H_8O_3$ on the phase change temperature, orthogonal experiments are used to select proper PCM. The levels and factors of orthogonal experiments are shown in Table 2. It shows that the NaCl solutions and $C_3H_8O_3$ solutions have two levels and the corresponding mass concentrations are 25% and 20%, and the mass mixing ratio of these two solutions is 3:2 and 1:1. The orthogonal experiments design is shown in Table 3.

Table 2. The factors and levels of orthogonal experiments

Level	NaCl concentration	$C_3H_8O_3$ concentration	Mixing ratio
I	25%	25%	3:2
II	20%	20%	1:1

Table 3. The orthogonal experiments design

Sample No.	NaCl concentration (wt. %)	$C_3H_8O_3$ concentration (wt. %)	Mixing ratio
1#	I 25%	I 25%	I 3:2
2#	II 20%	I 25%	II 1:1
3#	I 25%	II 25%	II 1:1
4#	II 20%	II 25%	I 3:2

Based on orthogonal experiments design, experiments are conducted to measure the phase change temperature of the PCM. As shown in Table 4, the higher the concentration of NaCl and $C_3H_8O_3$ is, the lower the phase change temperature is, and the influence of $C_3H_8O_3$ concentration is

greater than that of NaCl. Therefore, the concentrations and mixing ratio are gradually adjusted under the guidance of the above experimental results. Finally, three kinds of PCMs are obtained, as shown in Table 5. The phase change temperatures of the three PCMs are all below -18 °C, but PCM3 possesses a larger latent heat than PCM1 and PCM2. Therefore, PCM3 is selected as a suitable material for the subsequent experiments.

Table 4. Results analysis of orthogonal experiments

Sample No.	NaCl concentration (wt. %)	$C_3H_8O_3$ concentration (wt. %)	Mixing ratio	Phase change temperature (°C)
1#	I 25%	I 25%	I 3:2	-13.29
2#	II 20%	I 25%	II 1:1	-13.46
3#	I 25%	II 25%	II 1:1	-11.77
4#	II 20%	II 25%	I 3:2	-9.30
Phase change temperature (°C)	I -25.06	-26.75	-22.59	\
	II -22.76	-21.07	-25.23	\
Range	2.3	5.68	2.64	\

Notice: The "range" is used to measure the effect of factors in the orthogonal experiments, and larger range means the corresponding factor has more effect on the experiment results.

Table 5. Experimental results under different concentrations of $C_3H_8O_3$ and NaCl

	$C_3H_8O_3$: NaCl: Water	Phase change temperature	Latent heat (kJ kg^{-1})
PCM1	10%:18%:72%	-21.6	106.1
PCM2	12%:18%:70%	-23.1	109.7
PCM3	15%:12.5%:72.5%	-18.2	138.4

4.2. Filling ratio optimization

The working fluid filling ratio has a great effect on the performance of the CTPLT. Insufficient filling ratio decreases the liquid film coverage in the evaporator resulting in heat transfer deterioration. While too much working fluid will increase the thickness of the liquid film, which increases the heat transfer resistance and reduces the heat transfer performance (Louahlia-Gualous et al., 2017). Therefore, it is important to determine the optimal filling ratio for the system to maximize its thermal performance.

To determine the optimal fill ratio, experiments are conducted under different fill ratios. The ambient temperature is set at 16.0 °C. T_{fre} represents the temperature of the fresh food compartment and it equals to the average value of T_{top} and T_{mid} according to the national standard for testing the domestic refrigerator. The temperature decreasing curves of T_{fre} under different filling ratios are shown in Fig. 4. The results show that the temperature decreasing trends are similar in the first 5.0 min because the temperature difference between the fresh food compartment and ambient temperature is minimum that the filling ratio has little effect on the T_{fre}. When the time on the horizontal axis in Fig. 4 is the same, the minimum temperature is achieved when the filling ratio is 27.0%. Fig. 5 shows the temperature decreasing time for various filling ratios when T_{fre} drops from

16 °C to 8.0 °C, 6.0 °C, and 4.0 °C, respectively. It indicates that the temperature decreasing time drops firstly and then rises with the increase of filling ratios, and it gets the minimum when the filling ratio is 27.0%. When the filling ratio is low, insufficient working fluid will lead to overheating at the outlet of the evaporator and undercooling at the outlet of the condenser. The two-phase heat transfer area with the highest heat transfer coefficient is short, which results in a poor heat transfer performance. If the filling ratio increases too much, the two-phase heat transfer in the evaporator section is disturbed by the excess liquid working fluid, which also leads to the decrease of the heat transfer capability. Optimal heat transfer performance is obtained when the filling ratio is 27%. From the above-mentioned discussion, the optimal filling ratio for the experimental platform is 27.0%. Besides, the optimal filling ratio of the designed CTPLT is relatively low compared to other literature results. On the one hand, the diameter of the evaporator section (as shown in Fig .2) is considerably smaller than that of the other sections in the novel designed CTPLT, so the evaporator requires a small amount of working fluid. On the other hand, the heat transfer rate of the CTPLT is relatively low when it is applied to the temperature control of the fresh food compartment. And the internal flow of the working fluid is slow, small liquid level difference can drive the internal circulation of the CTPLT, which means the liquid line will not be filled with liquid. On the whole, the CTPLT requires less quantity of the R407c due to its special structural design.

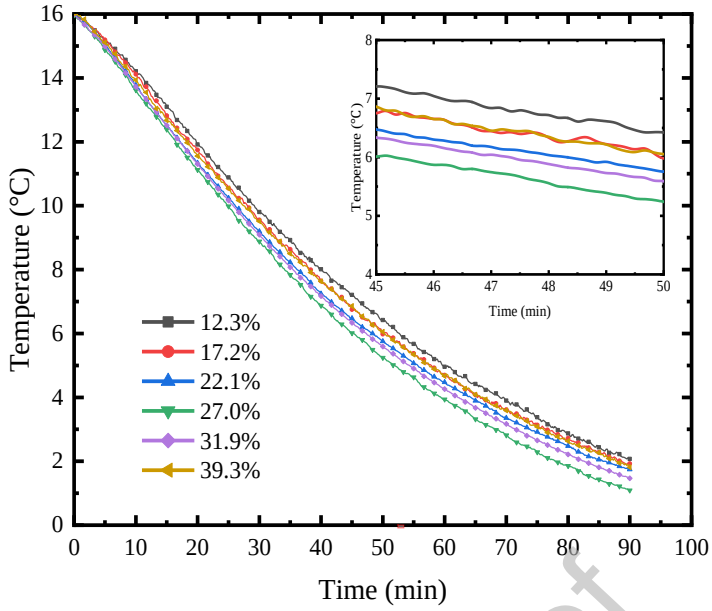

Fig. 4. Temperature decreasing curves under different filling ratios

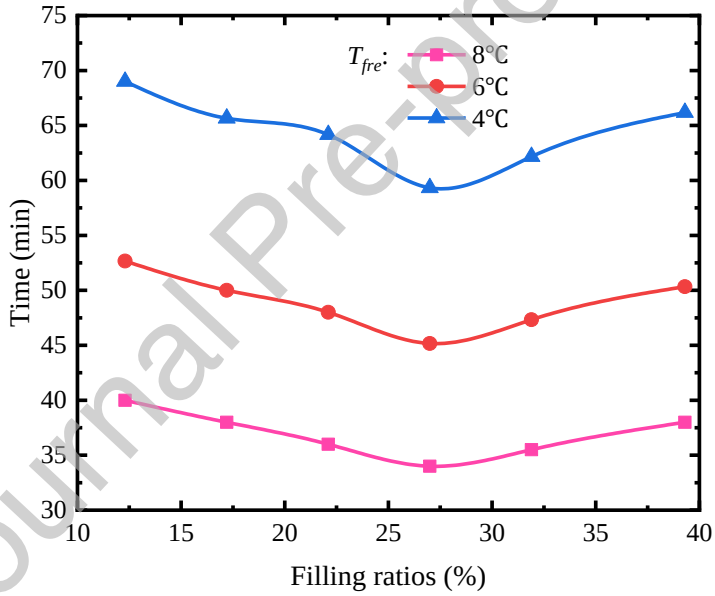

Fig. 5. Temperature decreasing time under different filling ratios and T_{fre}

4.3. Temperature regulation

Based on the aforementioned optimal filling ratio, the temperature adjustment capacity of the CTPLT on the fresh food compartment is further studied by temperature regulation experiments. The magnetic valves, which are regulated by the temperature controller, are used to control the internal flow and heat transfer of the CTPLT. The T_{fre} fluctuates around a certain value, T_{fre_ave}. T_{fre_ave} ranges from 2.0 °C to 8.0 °C. Fig. 6 particularly describes the stable operating states of CTPLT and T_{fre} when the T_{fre_ave} is 2.0 °C, 5.0 °C, and 8.0 °C, respectively. As illustrated in Fig. 6, T_{fre} can fluctuate stably within the upper and lower temperature limits with a certain T_{fre_ave}. The corresponding upper temperature limits are approximately 2.3 °C, 5.3 °C, and 8.3 °C when T_{fre_ave} is 2.0 °C, 5.0 °C, and 8.0 °C, respectively. The corresponding lower temperature limits are approximately 1.7 °C, 4.7 °C and 7.7 °C. It means that the temperature amplitude for T_{fre} is about 0.6 °C. Meanwhile, the variations in the working pressures of the CTPLT are periodic along with the on/off states. Table 6 shows the variations of working pressures at various T_{fre_ave}, indicating that the working pressure decreases with the increase of T_{fre_ave}. As T_{fre_ave} increases, the cold loss of the fresh food compartment is reductive and it results in the decline of the cold energy input of the fresh food compartment, which is conducive to reducing the operating temperatures and working pressures of the CTPLT. the decline of the cold energy input from CTPLT to the fresh food compartment

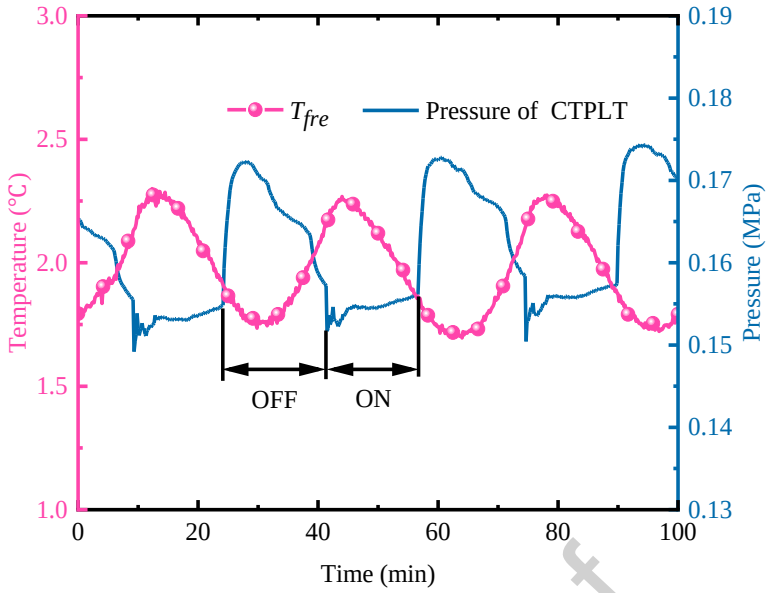

(a) T_{fre_ave} is 2.0 ℃

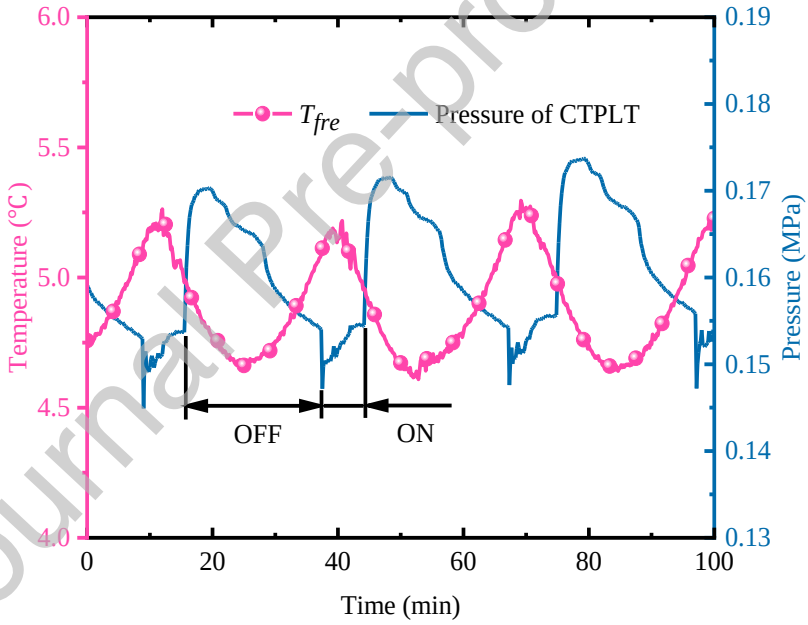

(b) T_{fre_ave} is 5.0 ℃

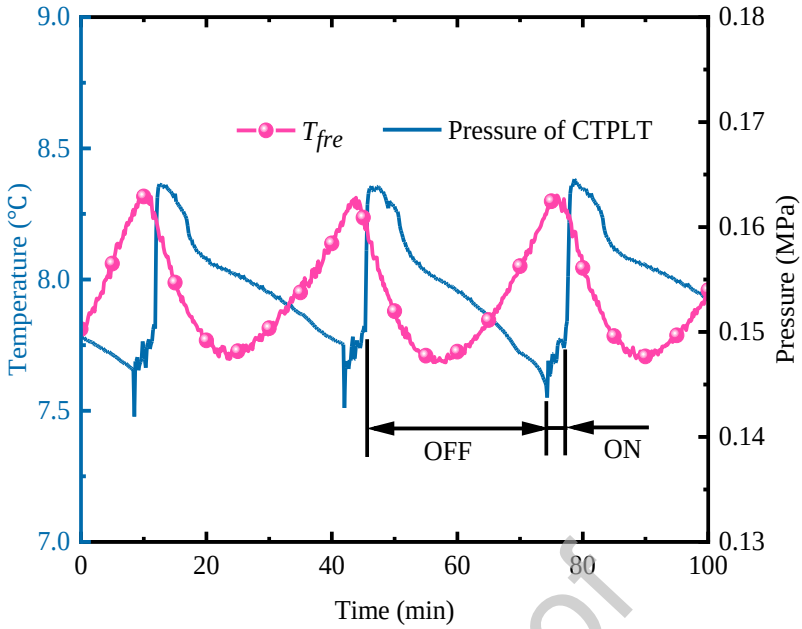

(c) T_{fre_ave} is 8.0 °C

Fig. 6. Stable operating states of T_{fre} and CTPLT at various T_{fre_ave}

Table 6. Working pressures at various T_{fre_ave}

Pressure (kPa)	T_{fre_ave} (°C)		
	2	5	8
Average working pressure	162	159	153
Highest working pressure	173	171	163
Lowest working pressure	151	147	143

Meanwhile, the on-off behaviors of the CTPLT at different T_{fre_ave} are analyzed in Fig. 7. The overall time refers to the time of one on-off cycle and its value is equal to the sum of operating time and stopping time. It is indicated that the overall time approximately maintains at 32.0 min, which demonstrates that T_{fre_ave} has little effects on the overall time of CTPLT under a certain temperature control accuracy. The heat load of the fresh food compartment increases as T_{fre_ave} decreases from

8.0 °C to 2.0 °C, the CTPLT needs to take more operating time to cool the fresh food compartment (the operating time increases from 3.9 min to 15.2 min as T_{fre_ave} decreases from 8.0 °C to 2.0 °C). In the meantime, the increases of the heat load will bring about an increase in the temperature rising rate of the fresh food compartment when the CTPLT stops working, the stopping time decreases with the decreases of T_{fre_ave} (the corresponding stopping time decreases from 28.6 min to 17.6 min). On the whole, the variations of T_{fre_ave} have opposite effects on the operating time and the stopping time of the CTPLT, and the overall time changes little as T_{fre_ave} changes from 8.0 °C to 2.0 °C. The operation ratio, which is defined as the ratio of operating time to stopping time, increases from 13.6% to 86.3% when T_{fre_ave} decreases from 8.0 °C to 2.0 °C. Considering that the cold loss of the fresh food compartment increases as the T_{fre_ave} decreases, the CTPLT needs to enhance the operation ratio to maintain a certain temperature of the fresh food compartment. In general, the CTPLT can adjust its operating states to maintain periodic fluctuation around certain operating states of the system. The designed system owns the temperature adjustment capacity by actively controlling the on-off behaviors of the CTPLT.

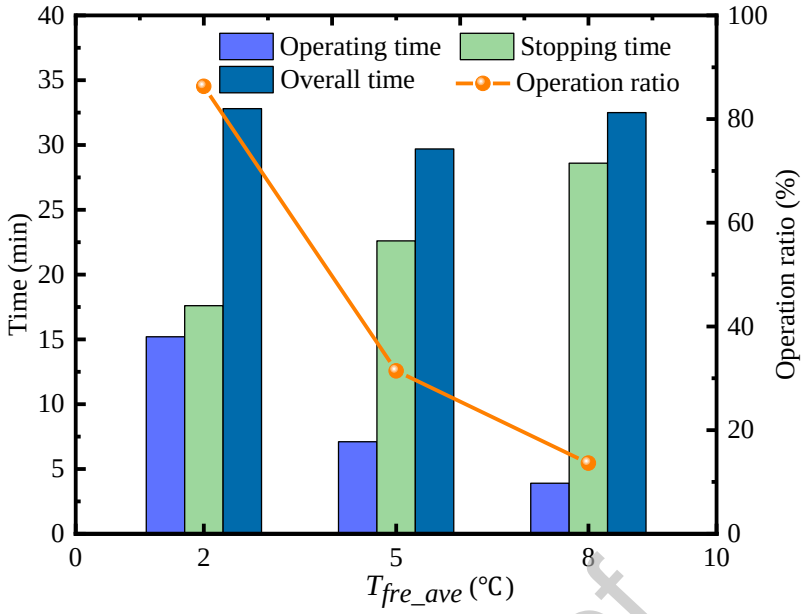

Fig. 7. On-off behaviors of CTPLT at different T_{fre_ave}

4.4. Adjustment of temperature control accuracy

In this section, further experiments were carried out to investigate the adjustment capacity of the temperature control accuracy of the CTPLT. The temperature difference (T_{diff}) that refers to the difference between the upper and lower temperature limits of the temperature controller was adjusted to change the on-off states of the CTPLT and the temperature fluctuations of T_{fre}. T_{fre_ave} is maintained at 5.0 ℃ throughout the experiments. Five working conditions with T_{diff} of 2.2 °C, 1.7 °C, 1.3 °C, 1 °C, and 0.7 °C were tested, and the behaviors of the fresh food compartment at T_{diff} of 2.2 °C, 1.3 °C, and 0.7 °C are selected for comprehensive discussion. As shown in Fig. 8, the results indicate that the temperature of the fresh food compartment varies periodically and stably, but the fluctuation amplitudes decrease with T_{diff}. Smaller temperature difference means an increase in the start and stop frequency of the CTPLT, which leads to a smaller range of temperature change. Meanwhile, the experimental results demonstrate that the temperature, T_{mid}, has the largest

amplitude among the three temperature measuring points. For instance, when T_{diff} is 1.7 °C, the temperature amplitude of T_{top}, T_{mid}, and T_{btm} is 0.6 °C, 0.7 °C and 1.5 °C, respectively. Hence the amplitude of T_{mid} can better represent the temperature control accuracy of the CTPLT. The temperature control accuracy is 2.1 °C, 1.3 °C, and 0.6 °C when T_{diff} is 2.2 °C, 1.3 °C, and 0.7 °C, respectively. Fig. 9 shows the fluctuation behaviors of the T_{fre} at different T_{diff}. The experiment phenomena indicate that the time for temperature rising, temperature dropping, and one temperature fluctuation cycle increases with T_{diff}. The temperature rising period is longer than the temperature dropping period. It can be explained that larger T_{diff} leads to the decline in the start-stop frequency, which means longer period of the temperature fluctuations. The results certificate that the temperature fluctuations of the fresh food compartment can be effectively adjusted by the CTPLT.

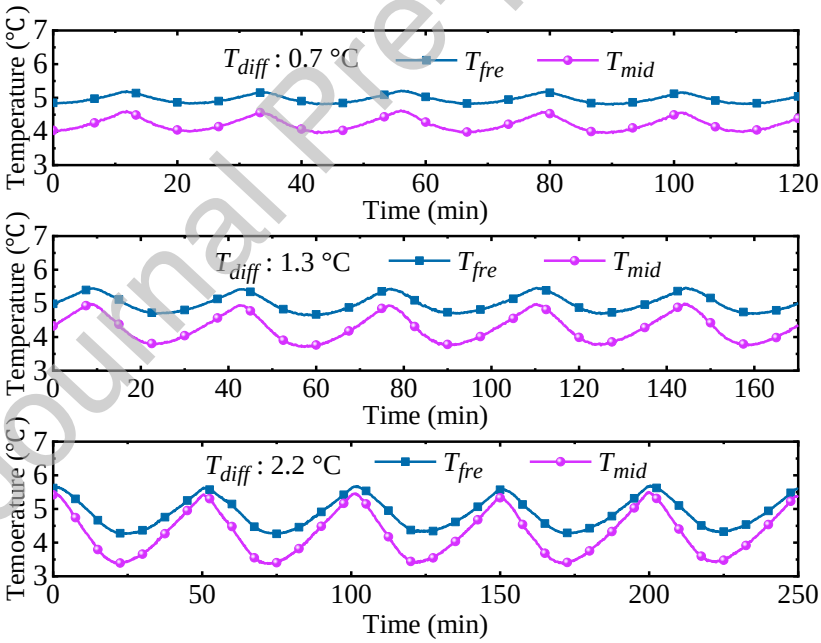

Fig. 8. Temperature fluctuation of the fresh food compartment at various T_{diff}

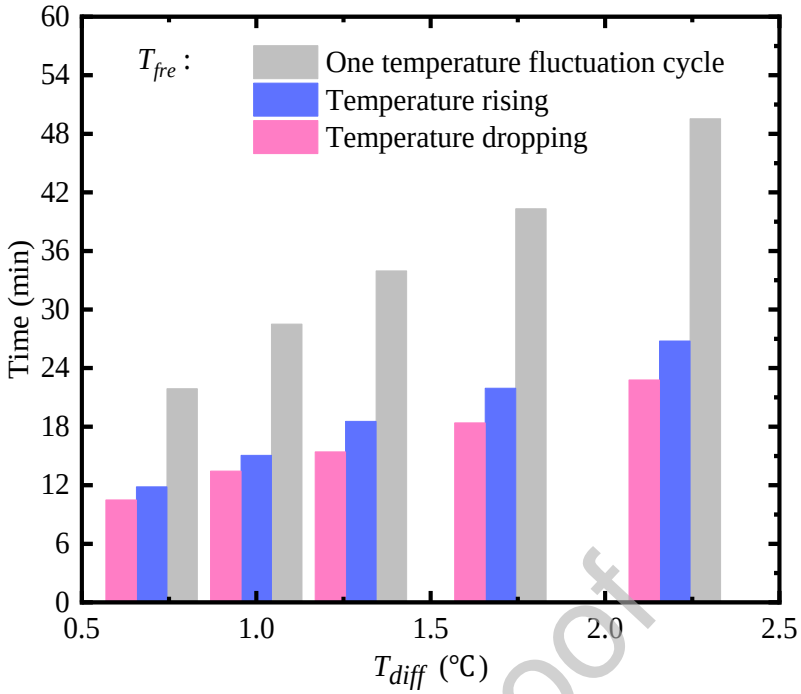

Fig. 9. Fluctuation behaviors of the T_{fre} at different T_{diff}

The on-off behaviors of the CTPLT and temperature control accuracy at different T_{diff} are shown in Fig. 10. It shows that the improvement of the temperature control accuracy is achieved from 2.1 °C to 0.6 °C as the T_{diff} decreases from 2.2 °C to 0.7 °C. The overall time of one on-off cycle decreases from 49.8 min to 22.4 min, and the operating time and stopping time of the CTPLT decrease with the decrease of T_{diff}, but the operation ratio gradually decreases from 48.4% to 19.25%, which implies that the heat transfer capacity enhances as T_{diff} decreases. In general, the temperature control accuracy of the fresh food compartment can change within a certain range by adjusting the temperature controller, and high-performance temperature controller is beneficial to achieve better temperature control accuracy. On the whole, a stable temperature control accuracy of 0.6 °C can be achieved, which is much higher than conventional domestic refrigerators (their normal accuracy is larger than 3 °C (Jofre et al., 2019)).

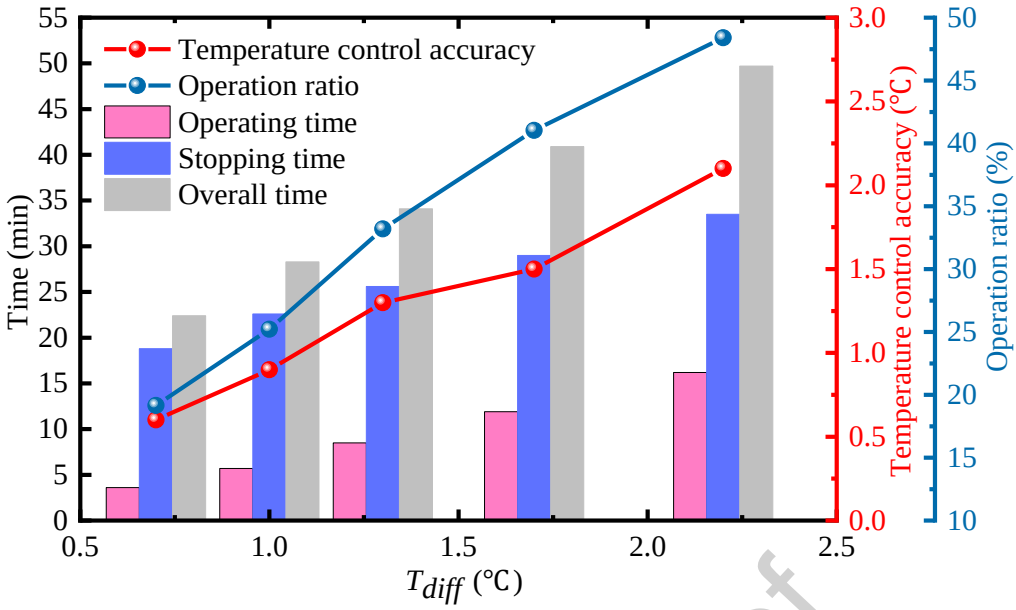

Fig. 10. On-off behaviors of CTPLT and temperature control accuracy at different T_{diff}

4.5. Effect of ambient temperature

To further investigate the effects of ambient temperature on the performance of temperature control, experiments were arranged under a range of temperatures in a constant temperature room with temperature control by a high-precision central air-conditioning. The experiments were carried out under ambient temperature of 16.0 °C, 18.0 °C, 20.0 °C, 22.0 °C, respectively. T_{fre_ave} is maintained at 7.0 °C throughout the experiments and the corresponding amplitude is 0.6 °C.

Fig. 11 presents the temperature variations in the fresh food compartment at different ambient temperatures. T_{top_ave} and T_{mid_ave} represent the average temperature when T_{top} and T_{mid} fluctuate with time. The temperature value of T_{mid_ave} is lower than that of the T_{top_ave}, which indicates that the heat transfer of the evaporator section has a greater impact on the middle region of the fresh food compartment. The liquid working fluid of the CTPLT is mainly distributed in the bottom area of the evaporator tube, and this area is mainly located in the rear wall surface of the middle region of the

fresh food compartment. Besides, due to the density difference, the cold air and hot air of the compartment will assemble in the middle region and top region, respectively. The T_{top_ave} and T_{mid_ave} change with the ambient temperature, but the overall change trend is not obvious, which means little effect of the ambient temperature on the temperature control. The temperature rising time and temperature dropping time of the T_{fre} show decreasing and increasing trends, respectively. As the ambient temperature increases, the heat transfer between the fresh food compartment and the ambient is enhanced, which will accelerate the temperature rising of the fresh food compartment as the CTPLT is off. Besides, more operating time is needed to provide cold energy for the cooling of the compartment as the CTPLT is on. Fig. 12 shows the on-off performance of CTPLT at different ambient temperatures. The overall time of one on-off cycle for the CTPLT maintains at approximately 35.0 min. As is mentioned in previous sections, the overall time of the CTPLT is related to the T_{diff} or temperature control accuracy. Meanwhile, the operating time increases from 2.3 min to 9.7 min and the stopping time decreases from 32.1 min to 21.1 min, which leads to a rise in operation ratio from 7.2% to 38.56% as the ambient temperature varies from 16.0 ℃ to 22.0 ℃. Increasing the ambient temperature leads to an increase of the temperature difference between the ambient and the fresh food compartment, which means the increase of the thermal load of compartment. The results indicate that the CTPLT can self-regulate its working states to control the temperature of the fresh food compartment at different temperatures, which further certificates its temperature control ability.

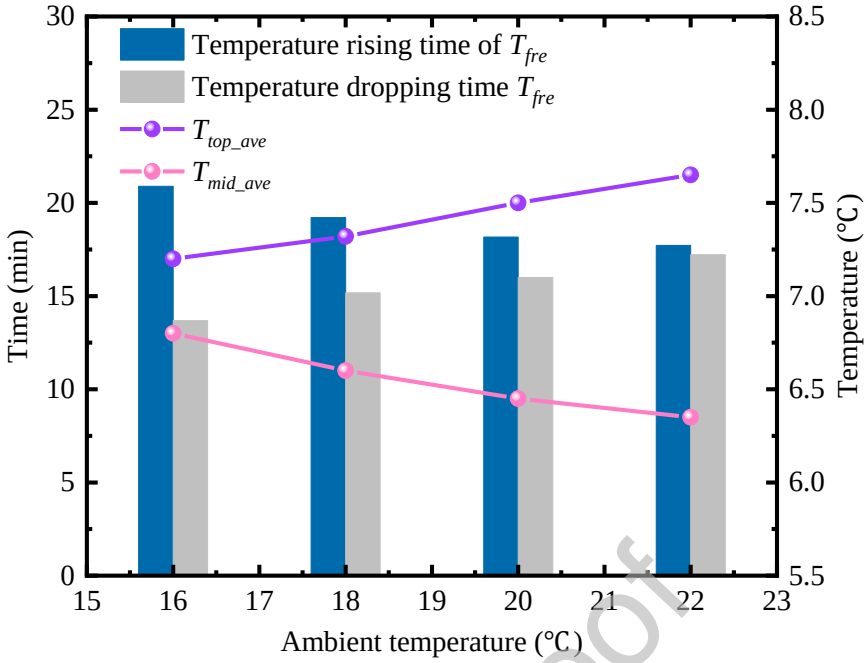

Fig. 11. Temperature variations of the fresh food compartment at different ambient temperatures

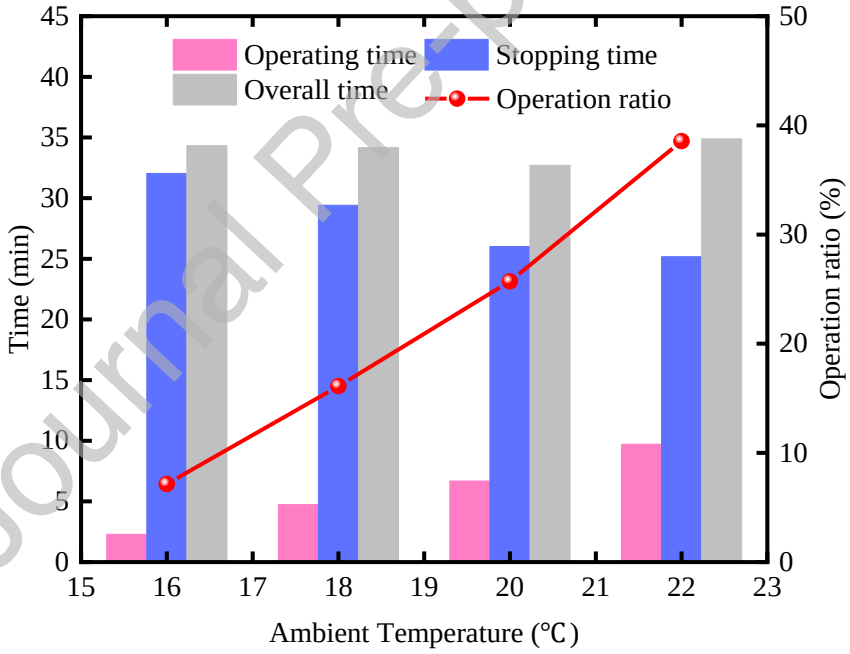

Fig. 12. On-off performance of the CTPLT at different ambient temperatures

5. Conclusions

In this study, a novel cool-storage refrigerator platform using a controllable two-phase loop thermosyphon as the precise temperature control device was designed. Experiments have been carried out to select suitable composite PCM and optimize the filling ratio of the working fluid. The capacities of the novel refrigerator in temperature regulation and the adjustment of temperature control accuracy were investigated. The effects of ambient temperatures on the working performance were finally studied. Following conclusions can be drawn:

1) Orthogonal experiments indicate that the concentration of $C_3H_8O_3$ has more effects on the thermal property of the composite PCM. One suitable PCM with the mass concentration ratio of $C_3H_8O_3$: NaCl: H_2O to be 15%: 12.5%: 72.5% is obtained by adjusting the concentration of its components step by step, and the corresponding phase change temperature and latent heat are -18.2 °C and 138.4 kJ kg^{-1}, respectively.

2) The temperature decreasing processes of the fresh food compartment at various filling ratios show that the T_{fre} reaches a minimum when the filling ratio is 27.0%. When T_{fre} drops from 16.0 °C to 8 °C, 6 °C, and 4 °C at various filling ratios, the smallest temperature decreasing time is obtained when the filling ratio is 27.0%. Thus, the optimal filling ratio of 27.0% is adopted for the following experiments.

3) As T_{fre_ave} varies from 2.0 °C to 8.0 °C, the variations of T_{fre} and the working pressure of controllable loop thermosyphon are stable and periodic. The overall time of one on-off cycle approximately maintains at 32.0 min, but the operating time decreases from 15.2 min to 3.9 min, which leads to the decrease of operation ratio from 86.3% to 13.6%. It is demonstrated that the

novel refrigerator can adjust the temperature of the fresh food compartment according to actual usage requirements.

4) When T_{diff} gradually decreases from 2.2 ℃ to 0.7 ℃, the overall time of one on-off cycle decreases from 49.8 min to 22.4 min, and the operation ratio gradually decreases from 48.4% to 19.25%. Besides, the improvement of the temperature control accuracy is achieved from 2.1 ℃ to 0.6 ℃, which is much better than that of the traditional domestic refrigerator.

5) When the ambient temperature rises from 16.0 ℃ to 22.0 ℃, the overall time of one on-off cycle is about 35 min, but the operating time rises from 2.3 min to 9.7 min, which demonstrates that the controllable two-phase loop thermosyphon can self-regulate its working states to maintain the temperature of the compartment at a certain value at different ambient temperatures.

All the results confirm the feasibility of the cool-storage refrigerator with the controllable loop thermosyphon. The designed cool-storage refrigerator has excellent temperature control performance, which would own a reference significance for the improvement of efficient refrigerator.

Declaration of interests

☒ The authors declare that they have no known competing financial interests or personal relationships that could have appeared to influence the work reported in this paper.

Acknowledgments

The study was sponsored by the National Key R&D Program of China (2018YFB1900602), the Anhui Provincial Natural Science Foundation (2008085QE234), the China Postdoctoral Science Foundation (2019M652209), the Fundamental Research Funds for the Central Universities (WK2090130024), and the National Natural Science Foundation of China (NSFC 51761145109 and 51776193).

References

Alam, M., Zou, P.X.W., Sanjayan, J., Ramakrishnan, S., 2019. Energy saving performance assessment and lessons learned from the operation of an active phase change materials system in a multi-storey building in Melbourne. Applied Energy 238, 1582-1595.

Bai, Y., Wang, L., Zhang, S., Lin, X., Chen, H., 2019. Numerical analysis of a closed loop two-phase thermosyphon under states of single-phase, two-phase and supercritical. International Journal of Heat and Mass Transfer 135, 354-367.

Bakhshipour, S., Valipour, M.S., Pahamli, Y., 2017. Parametric analysis of domestic refrigerators using PCM heat exchanger. International Journal of Refrigeration 83, 1-13.

Cao, J., Chen, C., Su, Y., Leung, M.K.H., Bottarelli, M., Pei, G., 2019. Experimental study on the temperature management behaviours of a controllable loop thermosyphon. Energy Conversion and Management 195, 436-446.

Cao, J., Hong, X., Zheng, Z., Asim, M., Hu, M., Wang, Q., Pei, G., Leung, M.K.H., 2020a. Performance characteristics of variable conductance loop thermosyphon for energy-efficient building thermal control. Applied Energy 275.

Cao, J., Zheng, Z., Asim, M., Hu, M., Wang, Q., Su, Y., Pei, G., Leung, M.K.H., 2020b. A review on independent and integrated/coupled two-phase loop thermosyphons. Applied Energy 280.

Chauhan, A., Kandlikar, S.G., 2019. Characterization of a dual taper thermosiphon loop for CPU cooling in data centers. Applied Thermal Engineering 146, 450-458.

Chen, S., Yang, J., 2016. Loop thermosyphon performance study for solar cells cooling. Energy Conversion and Management 121, 297-304.

Elarem, R., Mellouli, S., Abhilash, E., Jemni, A., 2017. Performance analysis of a household refrigerator integrating a PCM heat exchanger. Applied Thermal Engineering 125, 1320-1333.

Elkholy, A., Kempers, R., 2020. Experimental investigation of geyser boiling in a small diameter two-phase loop thermosyphon. Experimental Thermal and Fluid Science 118.

Fu, W., Li, X., Wu, X., Zhang, Z., 2015. Investigation of a long term passive cooling system using two-phase thermosyphon loops for the nuclear reactor spent fuel pool. Annals of Nuclear Energy 85, 346-356.

He, H., Furusato, K., Yamada, M., Shen, B., Hidaka, S., Kohno, M., Takahashi, K., Takata, Y., 2017. Efficiency enhancement of a loop thermosyphon on a mixed-wettability evaporator surface. Applied Thermal Engineering 123, 1245-1254.

Hong, S., Tang, Y., Wang, S., 2018. An investigation on optimal external cooling condition for an ultra-thin loop thermosyphon-based thermal management system. Energy Conversion and Management 172, 328-342.

Jafari, D., Franco, A., Filippeschi, S., Di Marco, P., 2016. Two-phase closed thermosyphons: A review of studies and solar applications. Renewable and Sustainable Energy Reviews 53, 575-593.

Jofre, A., Latorre-Moratalla, M.L., Garriga, M., Bover-Cid, S., 2019. Domestic refrigerator temperatures in Spain: Assessment of its impact on the safety and shelf-life of cooked meat products. Food Res Int 126, 108578.

Khodabandeh, R., 2005. Pressure drop in riser and evaporator in an advanced two-phase thermosyphon loop. International Journal of Refrigeration 28, 725-734.

Kiseev, V., Sazhin, O., 2019. Heat transfer enhancement in a loop thermosyphon using nanoparticles/water nanofluid. International Journal of Heat and Mass Transfer 132, 557-564.

Kondou, C., Umemoto, S., Koyama, S., Mitooka, Y., 2017. Improving the heat dissipation performance of a looped thermosyphon using low-GWP volatile fluids R1234ze(Z) and R1234ze(E) with a super-hydrophilic boiling surface. Applied Thermal Engineering 118, 147-158.

Li, X., Li, J., Zhou, G., Lv, L., 2020. Quantitative analysis of passive seasonal cold storage with a two-phase closed thermosyphon. Applied Energy 260.

Liu, Y., Li, Z., Li, Y., Jiang, Y., Tang, D., 2019. Heat transfer and instability characteristics of a loop thermosyphon with wide range of filling ratios. Applied Thermal Engineering 151, 262-271.

Louahlia-Gualous, H., Le Masson, S., Chahed, A., 2017. An experimental study of evaporation and condensation heat transfer coefficients for looped thermosyphon. Applied Thermal Engineering 110, 931-940.

Maiorino, A., Del Duca, M.G., Mota-Babiloni, A., Aprea, C., 2020. Achieving a running cost saving with a cabinet refrigerator incorporating a phase change material by the scheduling optimisation of its cyclic operations. International Journal of Refrigeration 117, 237-246.

Marques, A.C., Davies, G.F., Maidment, G.G., Evans, J.A., Wood, I.D., 2014. Novel design and performance enhancement of domestic refrigerators with thermal storage. Applied Thermal Engineering 63, 511-519.

Nasef, H.A., Nada, S.A., Hassan, H., 2019. Integrative passive and active cooling system using PCM and nanofluid for thermal regulation of concentrated photovoltaic solar cells. Energy Conversion and Management 199.

Niyaj, D.S., Sapali, S.N., 2017. Performance Evaluation of a Domestic Refrigerator with a Thermal Storage Arrangement Using Propane as a Refrigerant. Energy Procedia 109, 34-39.

Omara, A.A.M., Mohammedali, A.A.M., 2020. Thermal management and performance

enhancement of domestic refrigerators and freezers via phase change materials: A review. Innovative Food Science & Emerging Technologies 66.

Pirvaram, A., Sadrameli, S.M., Abdolmaleki, L., 2019. Energy management of a household refrigerator using eutectic environmental friendly PCMs in a cascaded condition. Energy 181, 321-330.

Shao, S., Liu, H., Zhang, H., Tian, C., 2019. Experimental investigation on a loop thermosyphon with evaporative condenser for free cooling of data centers. Energy 185, 829-836.

Tecchio, C., Oliveira, J.L.G., Paiva, K.V., Mantelli, M.B.H., Galdolfi, R., Ribeiro, L.G.S., 2017. Geyser boiling phenomenon in two-phase closed loop-thermosyphons. International Journal of Heat and Mass Transfer 111, 29-40.

Tong, Z., Liu, X.-H., Jiang, Y., 2017. Three typical operating states of an R744 two-phase thermosyphon loop. Applied Energy 206, 181-192.

Vikram, M.P., Kumaresan, V., Christopher, S., Velraj, R.J.I.J.o.R., 2019. Experimental studies on solidification and subcooling characteristics of water-based phase change material (PCM) in a spherical encapsulation for cool thermal energy storage applications. International Journal of Refrigeration 100, 454-462.

Watanabe, N., Phan, N., Saito, Y., Hayashi, S., Katayama, N., Nagano, H., 2020. Operating characteristics of an anti-gravity loop heat pipe with a flat evaporator that has the capability of a loop thermosyphon. Energy Conversion and Management 205.

Yan, C., Shi, W., Li, X., Wang, S., 2016. A seasonal cold storage system based on separate type heat pipe for sustainable building cooling. Renewable Energy 85, 880-889.

Yue, C., Zhang, Q., Zhai, Z., Ling, L., 2019. Numerical investigation on thermal characteristics and

flow distribution of a parallel micro-channel separate heat pipe in data center. International Journal of Refrigeration 98, 150-160.

Yusufoglu, Y., Apaydin, T., Yilmaz, S., Paksoy, H.O., 2015. Improving performance of household refrigerators by incorporating phase change materials. International Journal of Refrigeration 57, 173-185.

Zhang, H., Shao, S., Xu, H., Zou, H., Tang, M., Tian, C., 2017. Simulation on the performance and free cooling potential of the thermosyphon mode in an integrated system of mechanical refrigeration and thermosyphon. Applied Energy 185, 1604-1612.

Zhang, P., Wang, B., Shi, W., Li, X., 2015. Experimental investigation on two-phase thermosyphon loop with partially liquid-filled downcomer. Applied Energy 160, 10-17.

Zhang, T., Yan, Z., Pei, G., Zhu, Q., Ji, J., 2019. Experimental optimization on the volume-filling ratio of a loop thermosyphon photovoltaic/thermal system. Renewable Energy 143, 233-242.

Zhang, T., Yan, Z.W., Wang, L.Y., Zheng, W.J., Su, Y.H., 2020. Comparative study on the annual performance between loop thermosyphon solar water heating system and conventional solar water heating system. Solar Energy 197, 433-442.

Zhu, X., Li, X., Shen, J., Wang, B., Mao, Z., Xu, H., Feng, X., Sui, X., 2020. Stable microencapsulated phase change materials with ultrahigh payload for efficient cooling of mobile electronic devices. Energy Conversion and Management 223.

Zou, T., Fu, W., Liang, X., Wang, S., Gao, X., Zhang, Z., Fang, Y., 2018. Preparation and performance of modified calcium chloride hexahydrate composite phase change material for air-conditioning cold storage. International Journal of Refrigeration 95, 175-181.